IOP Publishing Superconductor Science and Technology
Supercond. Sci. Technol. 31 (2018) 125015 (10pp) https://doi.org/10.1088/1361-6668/aae4bc

Modeling methodology for a HTS flux pump using a 2D *H*-formulation

Jianzhao Geng and T A Coombs

Department of Engineering, University of Cambridge, Cambridge CB3 0FA, United Kingdom

E-mail: jg717@cam.ac.uk

Received 2 August 2018, revised 24 September 2018
Accepted for publication 27 September 2018
Published 8 November 2018

Abstract

Flux pumps are devices that can magnetize closed superconducting magnets in a gradual manner. High-T_c superconducting (HTS) flux pumps are particularly promising for high-field applications, due to the fact that lossless HTS coils are unavailable. The physics of these devices is also attractive. In this paper, we propose a modeling methodology for a transformer–rectifier HTS flux pump switched by dynamic resistance. A finite element model is built in Comsol and solved by a 2D *H*-formulation. The simulation result is verified by experimental data. The simulation will give a clear picture of how flux pumping occurs in a superconductor. It will show flux motion across a superconductor by shifting the electric central line, which is a unique feature of type-II superconductors. This work may be interesting in the understanding of magnetization of high-T_c superconductors.

Keywords: finite element model, HTS flux pump, 2D H-formulation, dynamic resistance, magnetization

(Some figures may appear in colour only in the online journal)

1. Introduction

Flux pumps are devices that can magnetize closed superconducting magnets without electrical contact. They are ideal alternatives to bulky electronic power sources in powering high-current high-field superconducting magnets. It is also tantalizing to understand the physics behind these devices where the concepts of flux motion, resistance, and electric field in the diamagnetic material are in line with Faraday's law [1].

Low-T_c superconducting flux pumps [2, 3] have been developed for decades. In these devices the superconductor is at least partially driven normal to allow flux motion. In high-T_c superconducting (HTS) flux pumps [4–8], however, it is not practical to drive the superconductor normal by magnetic fields, due to the very high irreversibility field [9] of high-temperature superconductors. In our previous work [10], we explained two ways for a HTS flux pump to work. The first [8] is to exceed the local critical current, either by inducting a current higher than the critical value, or by reducing the critical current density using an external field. The second [7] is to take advantage of the dynamic resistance effect [11–18]. When a type-II superconductor carrying a direct current is subjected to a perpendicular oscillating magnetic field, a vortex in the superconductor will redistribute and flux will travel across the superconductor. This effect occurs when the superconductor is fully penetrated by the transport current and the oscillating magnetic field. It should be noted that this effect is very different from the flux flow caused by de-pinning [19]. It is not necessary to exceed the local critical current density for flux to move. Therefore, this effect not only exists in superconductors with a nonlinear *E*–*J* curve (e.g. an *E*–*J* power law [20]), but also exists under the critical state model (CSM) [21], where the current density inside a superconductor can only be $\pm J_c$ or 0.

Recently, Campbell [22] proposed a finite element model to calculate flux pumping using a 2D *A*-formulation. His result showed that flux pumping occurs under the CSM, and the field dependence of J_c facilitates flux pumping. His result, however, did not show that flux pumping is associated with the dynamic resistance effect. In [23] and [24], a modeling technique for dynamic resistance was proposed using the *T*-formulation and *H*-formulation respectively. In this paper, we further these studies to show how dynamic resistance incurred flux pumping can be simulated using the *H*-formulation with finite element software. We will present a clear picture of how flux travels across a superconductor without transporting direct current.

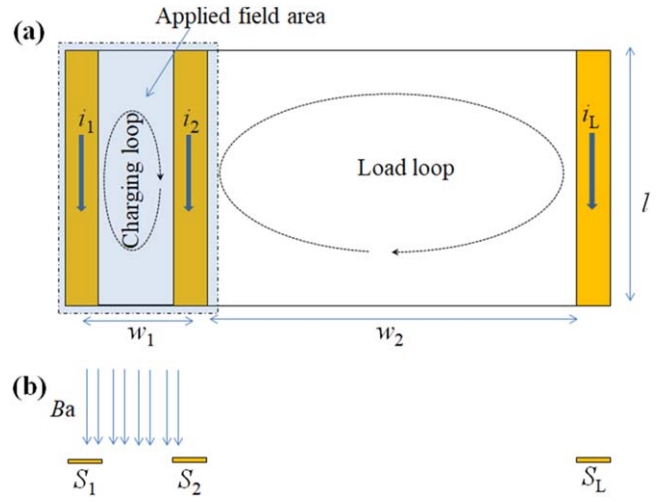

Figure 1. Schematic drawing of the HTS flux pumping circuit to be simulated. (a) Three thin superconducting strips (S_1, S_2, and S_L) are set in parallel with their terminations connected together. Two loops, a smaller charging loop and a larger load loop are formed. The field is applied perpendicular to the charging loop area. Flux pumping is considered to occur if the load loop current (i_L) is gradually charged up. (b) Cross section view.

2. Modeling methodology

2.1. Geometrical description

The circuit for the simulation consists of three parallel HTS strips, with their terminations connected together, as shown in figure 1(a). The three strips are denoted by S_1, S_2 and S_L respectively. The currents in these three strips are denoted by i_1, i_2, and i_L respectively, with the reference direction in figure 1(a). The closed loop formed by S_1 and S_2 is called the charging loop, which has a width of w_1. The third strip S_L is set far apart from S_1 and S_2. The loop formed by S_L and the other two strips is defined as the load loop, which has a width of w_2. The length of the three strips is denoted by l. We assume that the load loop is much larger than the charging loop, i.e. $w_2 \gg w_1$, and the length of the strips is much larger than the width of loops, i.e. $l \gg w_2$. We also assume that the magnetic field is applied only to the area of the charging loop, normal to the page, with a uniform field strength along l. Based on these assumptions, we may neglect the terminations of the strips, and can take an arbitrary cross section (normal to the strip length) for study, as shown in figure 1(b). Then the problem is converted to a 2D issue. The flux pumping effect is considered to happen if the magnetic field is only applied at the small charging loop area, and the load loop can be magnetized (i_L gradually increases).

We built a 2D infinitely long (into the page) model in Comsol PDE, the geometry is shown in figure 2.

The width of the HTS strips S_1 and S_2 is 12 mm each, and the width of S_L is 8 mm. S_1 and S_2 are 46 mm apart from each other, whereas S_L is about 360 mm away from S_2. It should be noted that in figure 2 the distance between S_2 and S_L is shortened for convenience.

Only the superconducting layer is simulated, and other layers (substrate, stabilizer, buffer layers) are neglected. The thickness of each strip is chosen to be 100 μm, which is 100 times the real thickness. The thickness enlargement will sacrifice accuracy but will not change the fundamentals.

Three electromagnets are used to apply fields to the charging loop. Each electromagnet consists of a pair of windings and an iron core. The central magnet goes through the gap between S_1 and S_2, which acts as a transformer inducing circulating current around S_1 and S_2. Each of the left and right magnets consist of a top and bottom pole, with a 1 mm gap to fit in S_1 and S_2. Thus they can apply magnetic fields normal to the surface of S_1 and S_2, acting as switches. The magnetic fields generated by the left and right magnets are denoted by switching fields. The whole area for simulation is a 2 m × 2 m square, and the rest is considered to be free space.

A mapped mesh is used in the superconducting strips, with 50 elements uniformly distributed along the width of each strip, and five elements uniformly distributed along the thickness of each strip. In the rest of the area a free triangular mesh is used.

2.2. 2D H-formulation

For the proposed geometry, the 2D H-formulation [25–28] is used for the simulation. In the H-formulation, the magnetic field $\boldsymbol{H}$ is used to solve the Maxwell equation, i.e. Faraday's law (1) and Ampere's law (2). By substituting Ohm's law (3) and magnetic property (4) into equations (1) and (2), one can eliminate all variables except $\boldsymbol{H}$, and acquire equation (5).

$$\nabla \times \boldsymbol{E} = -\frac{\partial \boldsymbol{B}}{\partial t}, \tag{1}$$

$$\nabla \times \boldsymbol{H} = \boldsymbol{J}, \tag{2}$$

$$\boldsymbol{E} = \rho \boldsymbol{J}, \tag{3}$$

$$\boldsymbol{B} = \mu_0 \mu_r \boldsymbol{H}, \tag{4}$$

$$\frac{\partial(\mu_0 \mu_r \boldsymbol{H})}{\partial t} + \nabla \times (\nabla \times \rho \boldsymbol{J}) = 0, \tag{5}$$

where $\boldsymbol{E} = [E_z]$ represents the electric field, $\boldsymbol{B} = [B_x, B_y]$ is the flux density, $\boldsymbol{H} = [H_x, H_y]$ is the magnetic field strength, and $\boldsymbol{J} = [J_z]$ is the current density. ρ is resistivity, μ_0 is the permeability of free space, and μ_r is the relative permeability.

To solve equation (5), the relative permeability and resistivity are needed for each material. For the sub-domain of iron cores, the relative permeability is set to be $\mu_r = 1000$, and for all other subdomains $\mu_r = 1$. The resistivity of the air domain is set to be $\rho = 1\ \Omega$m, for iron subdomains it is set to be $\rho = 0.01\ \Omega$m, and for the winding subdomains it is set to be $\rho = 10^{-8}\ \Omega$m. The resistivity of superconductors follows the E–J power law [20]:

$$\boldsymbol{E} = E_0 \left(\frac{\boldsymbol{J}}{J_c} \right)^n, \tag{6}$$

where E_0 is 10^{-4} V m^{-1}, and $n = 21$. The value of J_c is set to be 2.5×10^2 A mm^{-2}, and the critical current is 300 A in strips S_1 and S_2, and 200 A in strip S_L. Here we intentionally do not consider any field dependence of the critical current

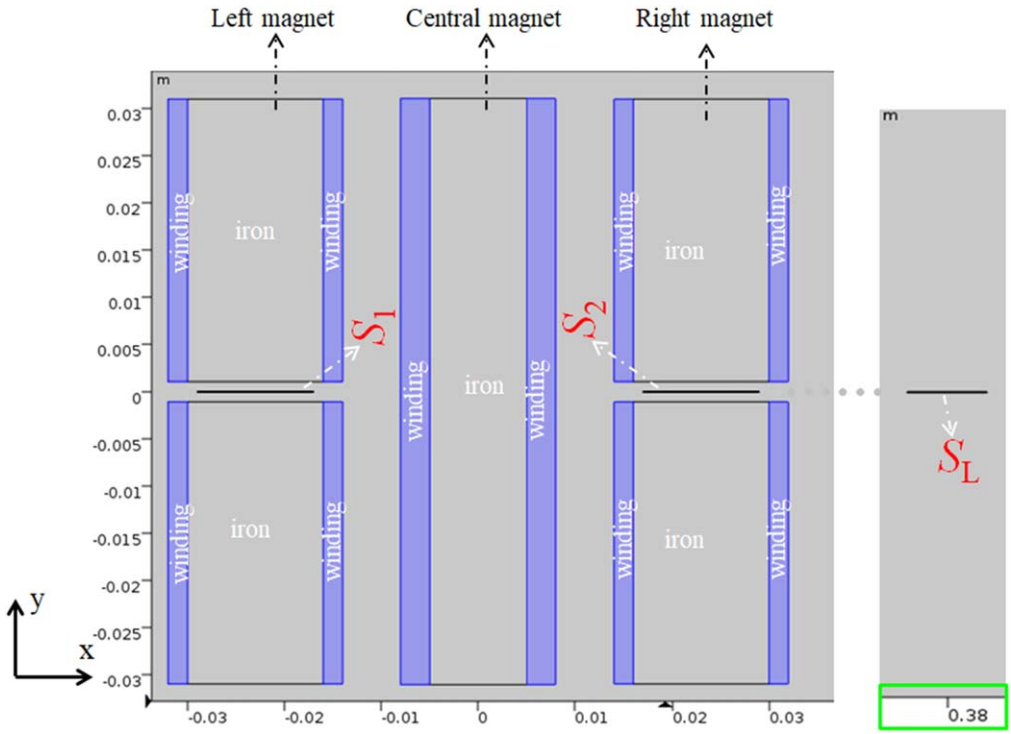

Figure 2. The 2D infinitely long model simulating flux pumping effect in Comsol. S_1, S_2 and S_L indicate the three HTS strips. The central electromagnet goes through the gap between S_1 and S_2, which is used to generate a circulating screening current in between S_1 and S_2. The left and right magnets are used to generate magnetic fields perpendicular to S_1 and S_2, referred as switching fields. It should be noted that the strip S_L is actually far away from the other two strips in the model, and in order to let readers view the geometry clearly they are shown close to each other.

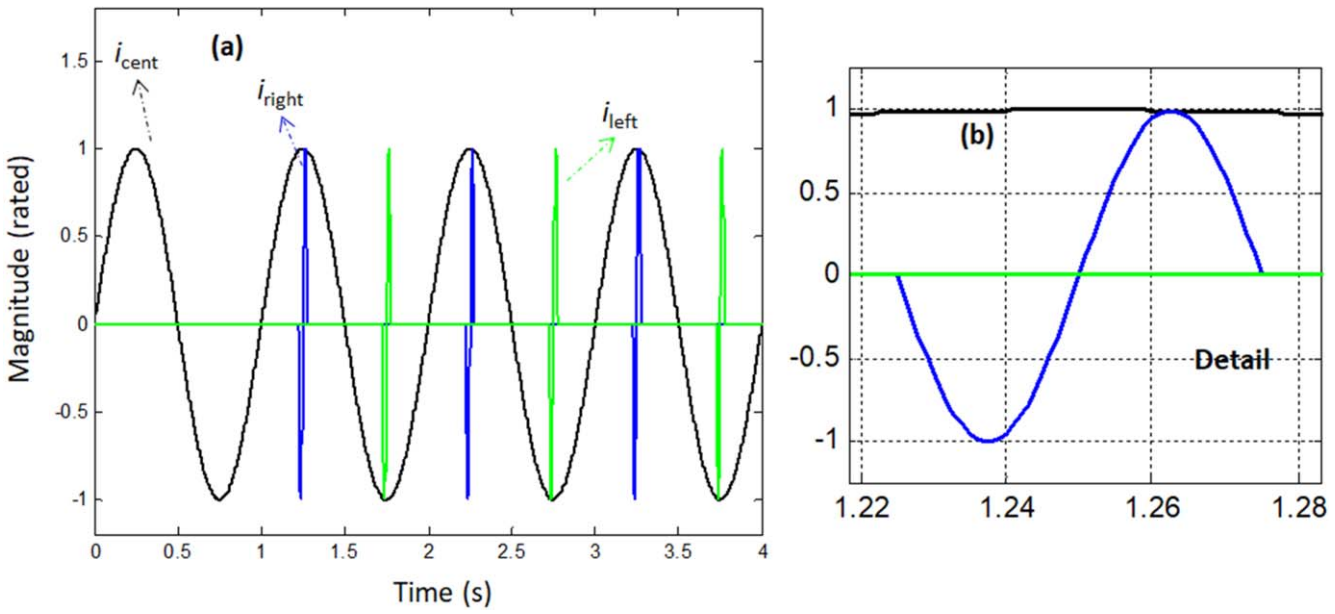

Figure 3. Waveform of the three currents driving the magnets. The central magnet is driven by a 1 Hz current, the right magnet is driven by an intermittent 20 Hz current which is only applied one cycle at each positive peak of the central magnet current, and the left magnet is driven by an intermittent 20 Hz current which is only applied one cycle at each negative peak of the central magnet current. (a) Overall waveform, (b) detail of one ac switching field cycle. (The current magnitudes do not reflect the actual value.)

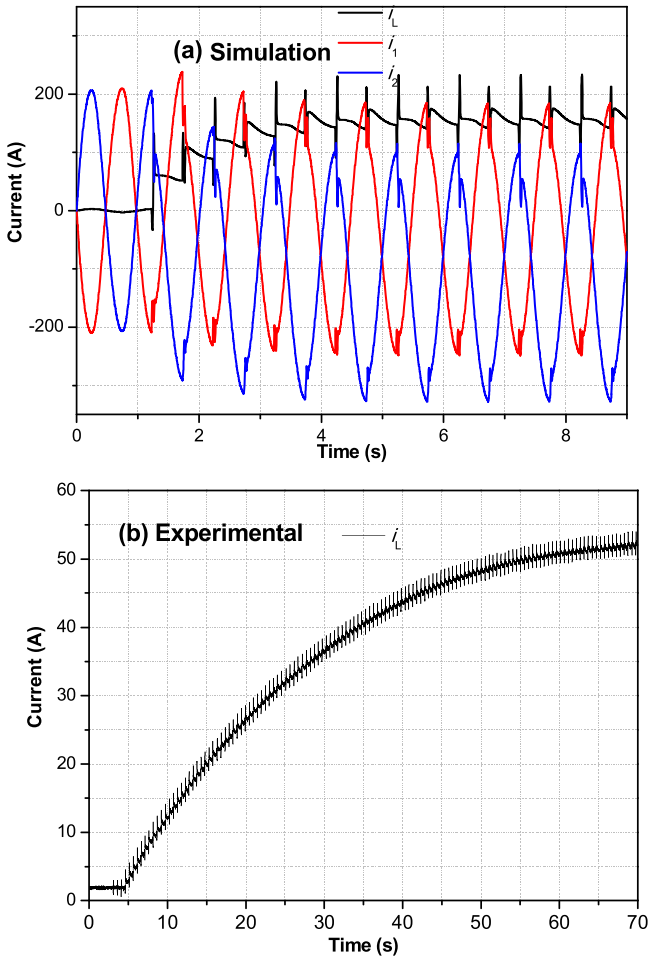

Figure 4. Simulation and experimental results showing flux pumping. (a) Simulation result showing the waveform of i_1, i_2, and i_L. (b) Experimental result showing the charging curve of a transformer–rectifier flux pump switched by dynamic resistance.

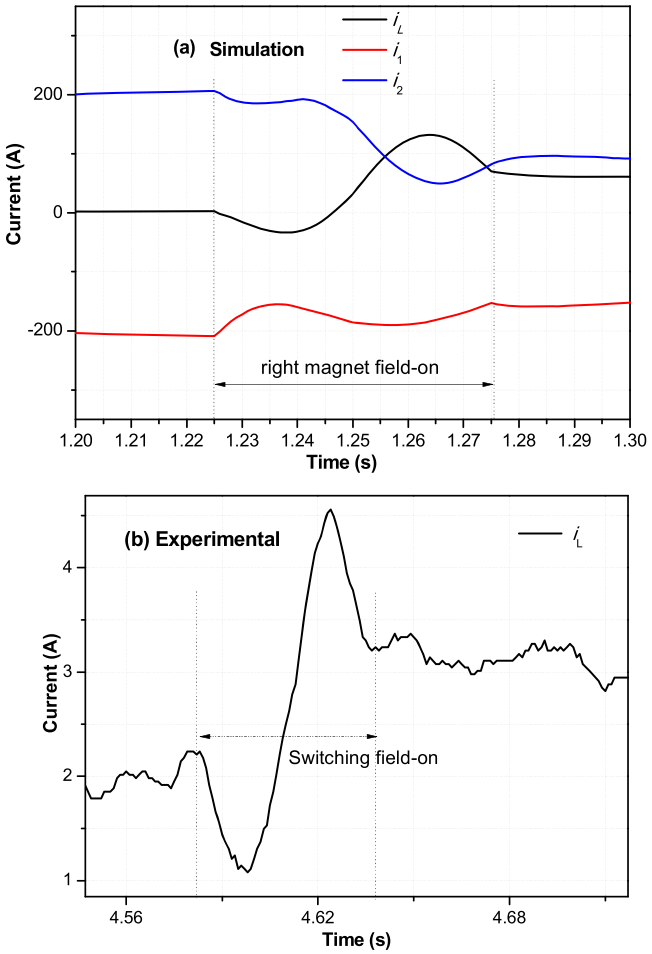

Figure 5. Simulation and experimental result comparison during a single period of the switching field. (a) Simulation result, (b) experimental result.

density. The aim is to show that pure dynamic resistance is sufficient to result in flux pumping. We want to distinguish this effect from the field dependence of the J_c induced flux pumping effect, which has been predicted [10] and experimentally verified [8] in our previous work, and numerically verified by Campbell [22].

The boundary condition for the superconductors is

$$\boldsymbol{i}_1 + \boldsymbol{i}_2 + \boldsymbol{i}_L = \int_{S1} \boldsymbol{J}\mathrm{d}S + \int_{S2} \boldsymbol{J}\mathrm{d}S + \int_{SL} \boldsymbol{J}\mathrm{d}S = 0. \quad (7)$$

Equation (7) indicates that although the current in each of the three superconducting strips is unknown, by forcing the sum of the three currents to be zero, the three superconductors are forming a circuit which looks like the one in figure 1(a). The boundary condition is achieved by using a point-wise constraint in the superconducting domains.

The outer boundaries which are far from the area of interest are set to be zero flux.

2.3. Generation of magnetic fields

Magnetic field is applied by setting the current in the windings, and each pair of windings wound around the same iron core have the same current magnitude but are opposite in direction (current flows in from one winding and flows out from the other). The top and bottom windings of the left (or right) magnet have the same current, so that

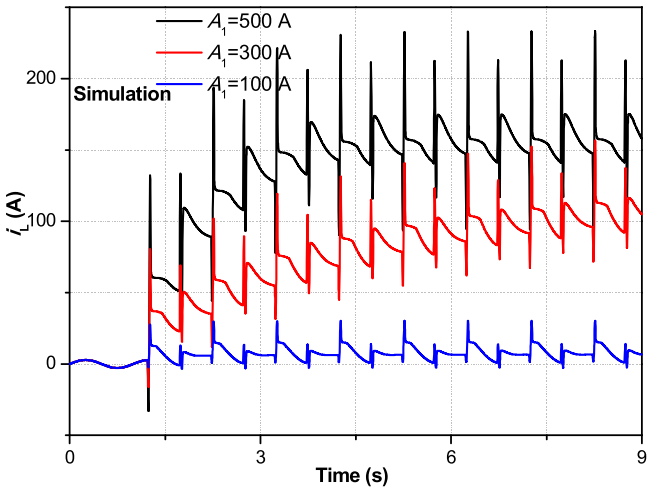

Figure 6. Simulation result of i_L ramping under different magnitudes of switching fields.

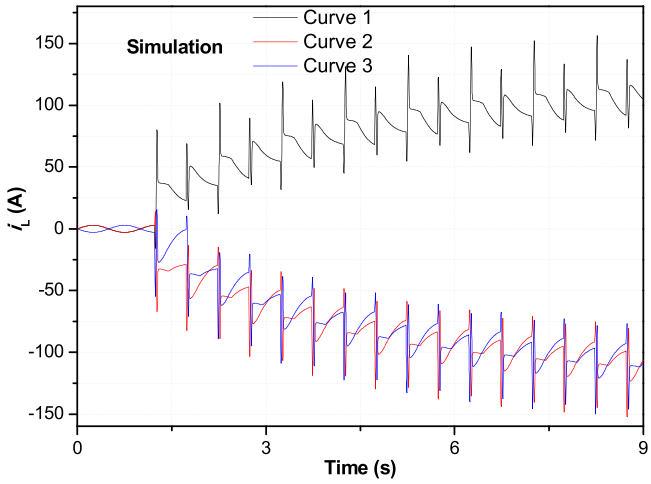

Figure 7. Simulation result of i_L ramping under different current sequences. In Curve 1, the switching sequence is the same as that described in equation (8); in Curve 2, the switching sequence of i_{left} and i_{right} changes whereas i_{cent} is unchanged, so that i_{left} and i_{right} are applied around the negative peaks of i_{cent}; in Curve 3, the switching sequence of i_{left} and i_{right} is unchanged, but the phase of i_{cent} changes 180° so that i_{left} and i_{right} are also applied around the negative peaks of i_{cent}. In all three instances the magnitude of i_{left} and i_{right} is 300 A, and the magnitude of i_{cent} is 900 A.

in each air gap the magnetic field is mainly normal to the superconducting strip. The current is applied by integrating the current density in each winding area, and constraining it to a certain value. Specifically, the left magnet current i_{left}, the central magnet current i_{cent} and the right magnet current i_{right} are set to be:

$$\begin{cases} \boldsymbol{i}_{left} = A_1 \times \sin(40\pi t), \text{ for } 0.725 < mod(t, 1) < 0.775 \text{ and } t > 1 \\ \boldsymbol{i}_{cent} = A_2 \times \sin(2\pi t) \\ \boldsymbol{i}_{right} = A_1 \times \sin(40\pi t), \text{ for } 0.225 < mod(t, 1) < 0.275 \text{ and } t > 1 \end{cases}, \quad (8)$$

where A_1 and A_2 represent the magnitudes.

The waveform of these currents is plotted in figure 3. The central magnet current is a 1 Hz pure sine wave. The current in the left and right magnet is zero, except for a single cycle of a 20 Hz sine wave which occurs at each positive and negative peak of the central magnet current. During the first second, only the central magnet current is applied. This is to verify that symmetrical current in the central magnet will not result in flux pumping if there is no switching field applied. In the following simulation, A_2 in equation (8) is adjusted to 900 A so that the induced screening current in S_1 and S_2 has around a 200 A peak value, and the switching magnet current is changeable.

It should be noted that the actual applied magnetic fields slightly lag the driving currents, because of the current distribution transience in the windings.

The model was run on a desktop computer with a 3.5 GHz CPU and 32 GB of memory. In each run, 9 s was simulated. Each run took about 70–120 h depending on different applied field magnitudes.

3. Simulation result and analysis

3.1. Charging curves

Figure 4(a) shows the current curves in the three superconducting strips, with the switching magnet current magnitude A_1 in equation (8) set to be 500 A. We can see that during the first second when only the central magnet is activated there is a screening current flowing around S_1 and S_2, and the current i_L in S_L is very small. After that, the switching magnetic fields are alternatively applied to either S_1 or S_2 when the screening current in the strip is approaching its positive peak. Each time the switching field is applied, there is a net increase in the load current i_L, although there is an oscillation. At the same time, the current in the switched strip drops sharply. With the load current i_L ramping up, each step of increase in i_L becomes smaller. The load current saturates at about 180 A which is close to the peak value of the screening current in strips S_1 and S_2 before applying the switching field. The i_L curve looks like the charging curve of a first-order circuit. Figure 4(b) shows the experimental charging curve of an AC field switched transformer–rectifier HTS flux pump [7, 29] for comparison. The experiment is different from the simulation in the following aspects: it was a half-bridge rectifier rather than a full-bridge one, only one switch was used rather than two, the transformer current was a triangular wave rather than a sine wave, the transformer and the switching magnet have limited length, and the load was a 40 turn coil rather than a single strip. Despite these differences, the simulation and experimental charging curves are similar except for the charging speed. In the experiment the load coil inductance is much higher than the inductance of the strip, so the charging time is significantly longer.

To investigate the details, we enlarged figure 4 to display the time of a switching field cycle, as shown in figure 5. The figure clearly shows that the simulation waveform is in accordance with the experimental data. After applying the switching field, there is an increase in the load current i_L.

We also investigated the influence of switching field magnitudes on the flux pumping performance. In the simulation we chose the value of A_1 in equation (8) to be 100 A, 200 A, and 500 A. As shown in figure 6, a higher field magnitude results in faster charging as well as a higher final saturation load current. When the switching field is too low, a very little load current is pumped, this is because the switching field can barely overcome the threshold field. This will be discussed in next section.

Another set of simulations is done concerning the flux pumping polarity which is considered important. The load current curves are shown in figure 7 under three different field application sequences. In Curve 1, the applying field sequence is

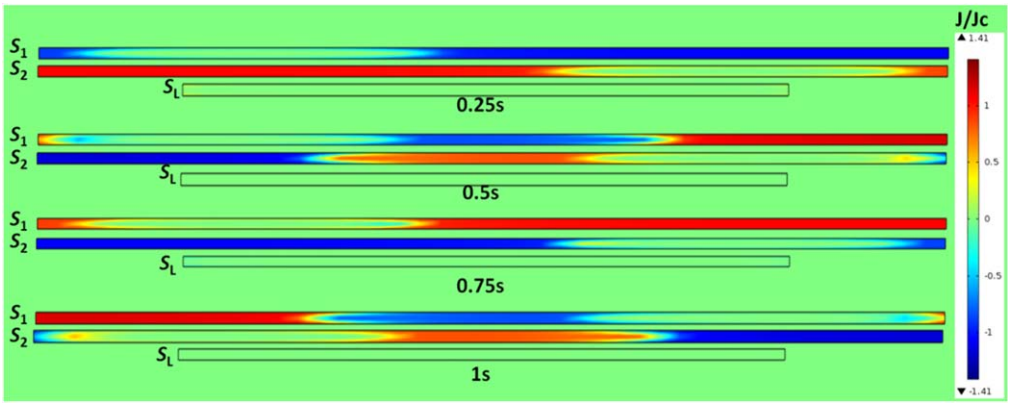

Figure 8. Current distribution in the three superconducting strips during the first cycle of the central magnet current changes. The time corresponds to the curve in figure 3. The thickness of each strip is intentionally enlarged to present a clearer view.

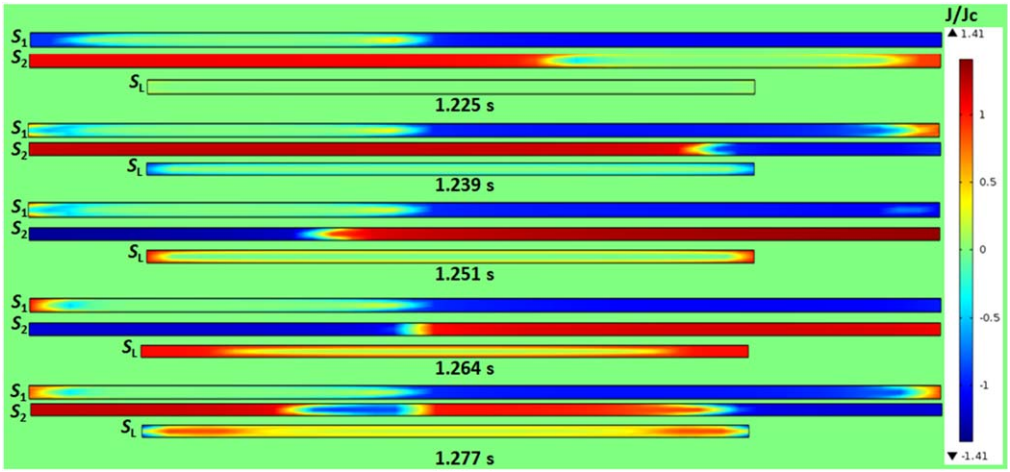

Figure 9. Current distribution in the three superconducting strips during the first cycle of applied field on S_2 by the right magnet.

the same as described in figure 3. In Curve 2, the current i_{cent} is the same as described in figure 3, but i_{left} and i_{right} change order. In this case, both i_{left} and i_{right} are applied around the negative peaks of i_{cent}. In Curve 3, the currents i_{left} and i_{right} are the same as described in figure 3, whereas the phase of i_{cent} changes by 180°, so that the currents i_{left} and i_{right} are also applied around the negative peaks of i_{cent}. The load current in Curve 2 and Curve 3 become negative, indicating the flux motion is only dependent on the direction of the screening current around strip S_1 and S_2 when the switching field is applied. This is in accordance with the classic dynamic resistance model. The minor difference between Curve 2 and Curve 3 is due to the fact that the geometry is not strictly symmetrical. The right magnet is closer to strip S_L than the left magnet, so the inductions of these two magnets are different.

3.2. Current and magnetic field distribution

To further understand the electromagnetic behavior in the superconductors, we investigated the current and magnetic field distribution in the strips. In all the following results, the thickness of each strip is intentionally enlarged for a clearer view.

Figure 8 shows the current distribution in the three superconducting strips during one cycle of the central magnet current, during which the left and right magnets are not activated. For the strips S_1 and S_2 which enclose the central magnet, most of the current tends to circulate the charging loop in the inner part, and only a little portion of the current flows near the edge. There is very little current flowing through the strip S_L because it is far away from the central magnet, and also the induction by the central magnet is shielded by the strip S_1 and S_2.

Figure 9 shows the current distribution in the three superconducting strips during the first cycle of applied field on the strip S_2. It is noted that the frequency of i_{right} is 20 Hz, so its duration is 0.05 s. However, there is a slight delay in the applied field compared to the current, because of transitional current redistribution in the windings. The current is applied from 1.225 to 1.275 s, whereas as the field response is from 1.225 to 1.277 s. At the time point of 1.225 s, the field has not been applied to the strip, so little current is flowing through S_L, and the currents in S_1 and S_2 look symmetrical. After this time point the switching field of S_2 starts to decrease to its negative peak at 1.239 s. During this period, a screening current induced by the switching magnet penetrates the strip

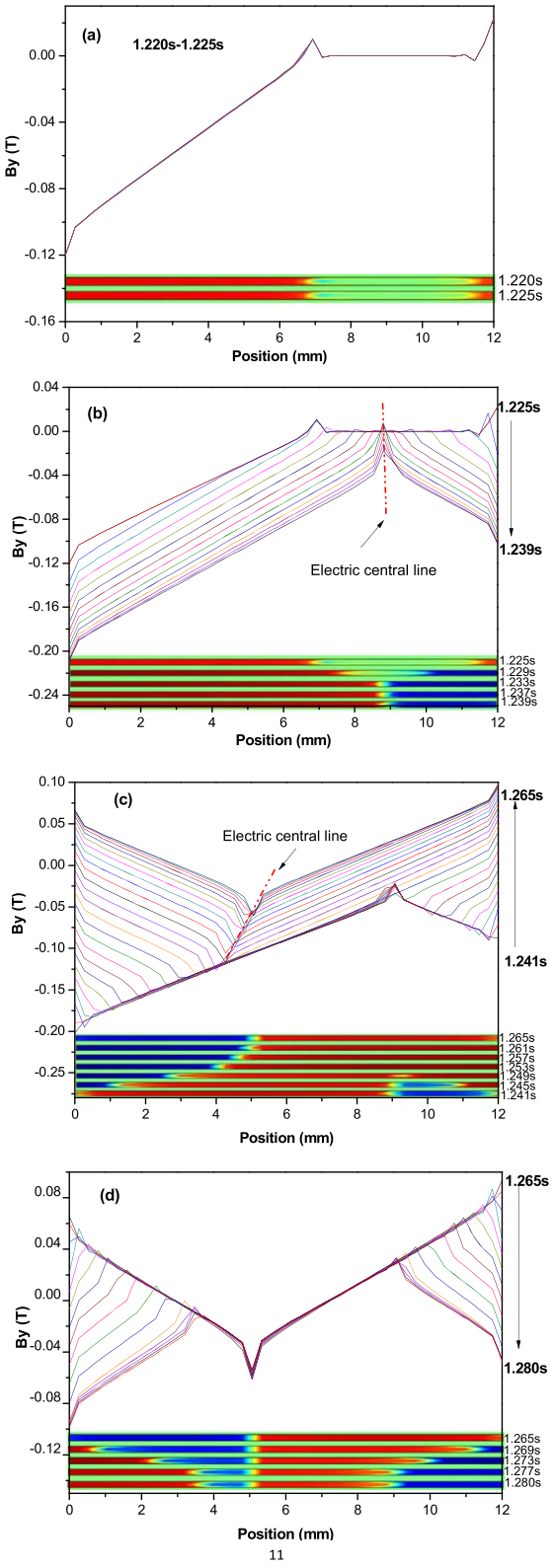

Figure 10. Current and magnetic field distributions in the strip S_2 during the time when field is applied to it. The position 0 mm indicates its left edge, and the position 12 mm indicates the right edge. The vertical magnetic flux density B_y is the value from the middle line of strip S_2 ($y = 0$) across its width. The magnitude of i_{right} is 500 A.

S_2 from both edges. Because the central magnet has already induced a current (it can be approximately considered a 'transport current') in the strip, the current distribution in the strip is not symmetrical. As can be seen from the 1.239 s scene in figure 9, the electric central line (the opposite side of which the electric field changes directions) in S_2 is biased to the right. Another detail worth paying attention to is that due to the flux penetration into the strip S_2, flux linking of the strip S_1 and S_L changes, resulting in a corresponding current change. The current in the strip S_1 changes color at both edges, indicating a current decrease; whereas a blue current occurs at the outer part of the strip S_L, also indicating a flux change. After 1.239 s, the applied field starts to increase, and the induced screening current changes direction. However, because of the existence of the 'transport current', the electric central line in the strip has been shifted to the left. It is clearly seen that at 1.25 s the current in S_L has changed direction, and at 1.264 s it increased to a noticeable value. The point at 1.264 s is when the applied field reaches its positive peak, and after that it decreases to zero at 1.277 s, completing an entire cycle. It can be seen that although the current in S_L has a slight decrease from 1.264 s to 1.277 s, its final value is still much larger than its initial value at 1.225 s, indicating flux pumping has been achieved. A similar result is observed when the field is applied to the strip S_1.

A clear picture of how flux has traveled across strip S_2 is shown in figure 10. The position of interest is chosen to be the middle line of strip S_2 ($y = 0$) across its width. The figure shows the flux density in the y (B_y) direction across the line, and the current distribution in it. The position 0 mm indicates the left edge of S_2 and the position 12 mm indicates the right edge of S_2.

Figure 10(a) shows the time period of 1.220 to 1.225 s, when the global screening current induced by the central magnets reaches its positive peak, and before the field is applied to S_2. During this time period the current is relatively stable, and mostly distributed in the left side. There is a virgin area in the strip where no current has penetrated in. The slope of the vertical magnetic flux density (B_y) is in accordance with the current distribution. In the virgin area, B_y is close to zero.

Figure 10(b) shows the time period of 1.225 to 1.239 s, when the field applied to S_2 changes from zero to negative maximum. The total flux in the strip (absolute value) increases. Flux enters the strip from both edges, but more from the left than the right because there is an initial 'transport current'. The screening current induced by the right magnet 'pushes' the initial current at the left side further into the strip, whereas it changes the current direction at the left side. At about 1.233 s, the strip is fully occupied by the initial 'transport current' and the screening current. The positive current and negative current meet at the position near the right edge, which is referred as the electric central line. After that, the screening current does not increase much with the increase of applied field.

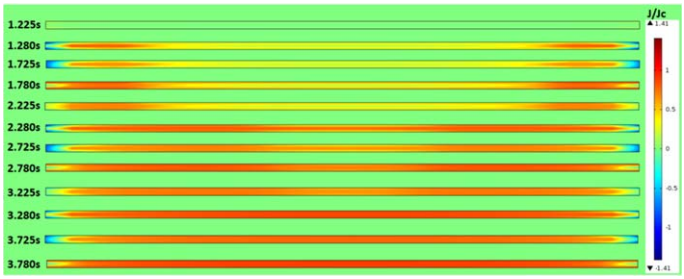

Figure 11. Current evolution in the strip S_L during muli-cycles of applied field.

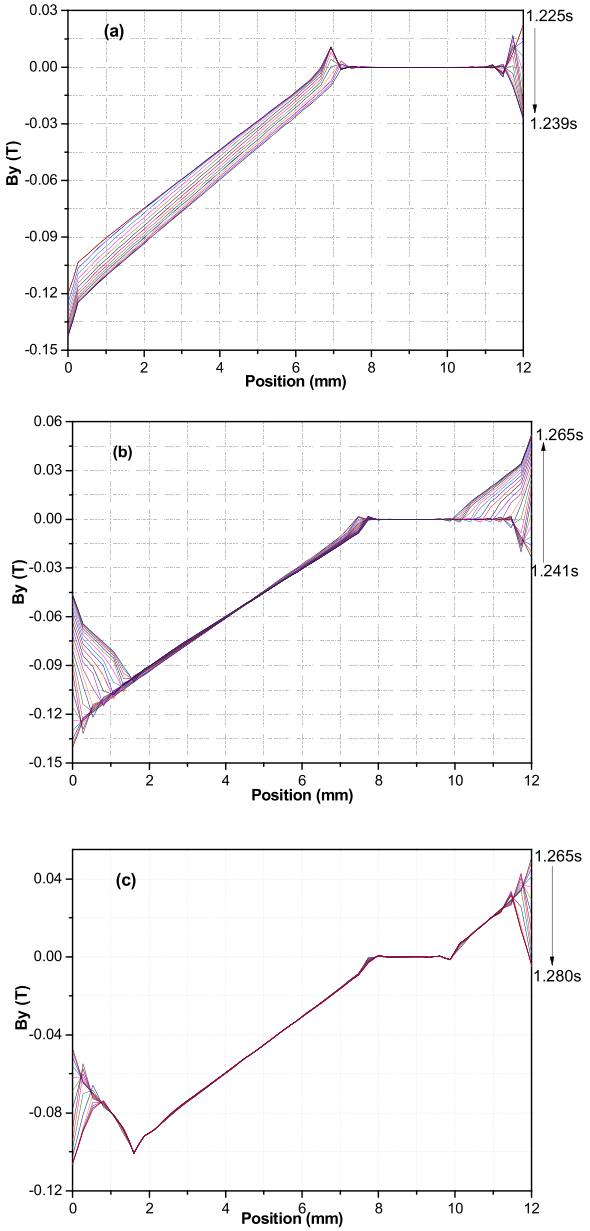

Figure 12. Magnetic field distributions in the strip S_2 when the switching field magnitude is under the threshold value. The magnitude of i_{right} is chosen to be 100 A.

Figure 10(c) shows the time period 1.241 to 1.265 s, when the field applied to S_2 increases from the negative maximum to the positive maximum. Before 1.249 s, the screening current changes direction at both edges, and the slope of B_y also changes near the edges. But in the center area both the current and B_y stay unchanged, seeming to be 'frozen'. The field change from 1.241 to 1.249 s can be considered as the threshold value [30, 31] in the dynamic resistance model, under which the applied field cannot interact with the transport current. At 1.249 s B_y changes at all positions of the strip. The electric central line has now been shifted to the left. But its position varies with the increase of the applied field. This is because the 'transport current' in the strip is not stable. It decreases when the field is applied to S_2, and also when some current has bypassed by S_L resulting in an increase in i_L.

Figure 10(d) shows the time period 1.265 to 1.280 s, when the field applied to S_2 decreases from the positive maxima to zero, during which time only the current and field near the edges change direction.

Comparing figures 10(b) and (c), we can clearly see that the electric central line has been shifted by the 'transport current' induced by the central magnet. Therefore, there is a net flux motion across the strip.

At the end of this section, we show the current evolution in S_L during the first few cycles of charging in figure 11.

3.3. Threshold magnetic field

Another issue which is of importance is the threshold field [30, 31], which is normally used to determine the minimum field to generate dynamic resistance. In the dynamic resistance model, transport current is assumed to flow in the central part of a strip, and the rectifying effect only occurs if the applied field is large enough to penetrate to the area of flowing transport current. Figure 12 shows a case in which the applied field is slightly lower the threshold value. During the whole cycle of the switching field, there is an area in the center of the tape (8–10 mm) staying in a 'virgin state', without a current or field. In this case, no flux tends to travel across the strip. However, if we look at the current distribution in S_L during this period in figure 13, we can still see a weak pumping effect. This may be caused by the following factors. The first is that the strip is thin, so that some current tends to flow at the top and bottom surfaces of the strip rather than penetrating from the left and right edges to the center in a slab geometry. This may result in a rectifying effect. The second is that the initial 'transport current' is flowing near the

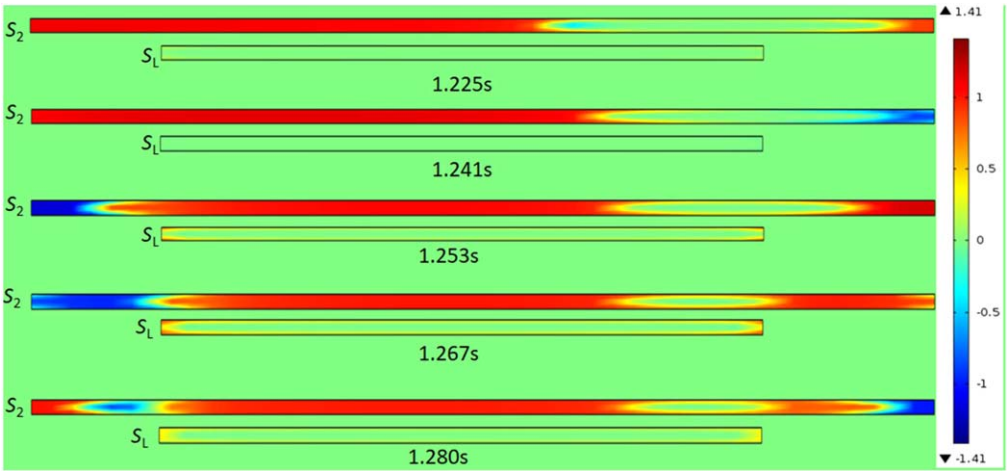

Figure 13. Current distribution when the applied field is close to the threshold value.

edges rather than in the center and the applied field can interact with it, changing the current and field distribution, hence the mutual induction between the charging loop and the load loop. In this case the 'pumped' current is more like a screening current rather than an injected current. The third is that the threshold field previously studied is based on static analysis, assuming that the field changing rate is infinitely slow, which is not the actual case in our simulation.

4. Discussion

Figure 10 clearly shows how flux can travel across an HTS strip. The central magnet induces a global screening current flowing around the charging loop formed by S_1 and S_2, and the left and right (the above result only shows the right) magnets induce a local screening current in an individual strip. If the strip is full of current, the local applied field interacts with the global screening current, resulting in a rectifying effect. This is very much similar to the well-known effect of dynamic resistance where a direct current carrying a type-II superconductor is under a perpendicular AC field. Although the induced global screening current is not a DC, its frequency in the simulation is much lower than the applied field frequency, so a similar effect can be seen. It is actually not necessary for the frequency of these two fields to be different from each other, and the rectifying effect occurs as long as the two fields are strong enough. Supposing that two magnetic fields are applied perpendicular to different parts of a thin strip, each of them tends to generate a screening current (inducing an electric field) in the superconductor. If these two magnetic fields are applied individually, the electric fields induced at a certain point of the superconductor may be different from each other. And if the fields are applied together, the electric field at the point cannot have two different values at the same time, which means there is a rectifying effect in the superconductor. In this case, it may be difficult to tell which is the magnetic field inducing the global 'transport current', and which is the switching field.

Overall, for flux pumping to work under a perpendicular field, the prerequisite is that the superconductor has to be thin. If the thickness is much larger than the width of the superconductor (slab geometry) or the radius of the loop formed by the superconductor (thick superconducting rings), flux pumping is less likely to happen because the inhomogeneous applied field will become homogeneous in the middle part of a superconductor due to the screening effect in the top and bottom surfaces. Thus the field distribution will follow Bean's model in the middle.

5. Conclusion

In this work, we proposed a finite element modeling method to simulate dynamic resistance switched transformer–rectifier flux pump using a 2D H-formulation. The simulation result is in accordance with our experimental data. The result has clearly shown how flux has traveled across an HTS strip without driving the superconductor normal. The model also shows that it is not necessary for the superconductor to be $J_c(B)$ dependent to achieve flux pumping, and indicates that the behavior may also occur in hard superconductors.

ORCID iDs

Jianzhao Geng https://orcid.org/0000-0002-0808-8567

References

[1] Giaever I 1966 *IEEE Spectr.* **3** 117
[2] van de Klundert L J M and ten Kate H H J 1981 *Cryogenics* **21** 195
[3] van de Klundert L J M and ten Kate H H J 1981 *Cryogenics* **21** 267
[4] Bai Z, Yan G, Wu C, Ding S and Chen C 2010 *Cryogenics* **50** 688
[5] Hoffmann C, Pooke D and Caplin A D 2011 *IEEE Trans. Appl. Supercond.* **21** 1628

[6] Jiang Z, Hamilton K, Amemiya N, Badcock R A and Bumby C W 2014 *Appl. Phys. Lett.* **105** 112601
[7] Geng J and Coombs T A 2015 *Appl. Phys. Lett.* **107** 142601
[8] Geng J and Coombs T A 2016 *Supercond. Sci. Technol.* **29** 095004
[9] Pardo E 2017 *Supercond. Sci. Technol.* **30** 060501
[10] Geng J *et al* 2016 *J. Phys. D: Appl. Phys.* **49** 11LT01
[11] Andrianov V V, Zenkevich V B, Kurguzov V V, Sychev V V and Ternovskii F F 1970 *Sov. Phys. JETP* **31** 815
[12] Huebener R P, Stafford L G and Aspen F E 1972 *Phys. Rev.* B **5** 3581
[13] Ogasawara T, Yasukochi K, Nose S and Sekizawa H 1976 *Cryogenics* **16** 33
[14] Risse M P, Aikele M G, Doettinger S G and Huebener R P 1997 *Phys. Rev.* B **55** 15191
[15] Rabbers J J, ten Haken B, Gomory F and ten Kate H H J 1998 *Physica* C **300** 1
[16] Oomen M P, Rieger J, Leghissa M, ten Haken B and ten Kate H H J 1999 *Supercond. Sci. Technol.* **12** 382
[17] Mikitik G P and Brandt E H 2001 *Phys. Rev.* B **64** 092502
[18] Uksusman A, Wolfus Y, Friedman A, Shaulov A and Yeshurun Y 2009 *J. Appl. Phys.* **105** 093921
[19] Yoshida Y, Uesaka M and Miya K 1994 *IEEE Trans. Magn.* **30** 3503
[20] Gladun A, Fuchs G, Fischer K, Busch D, Eujen R and Huedepohl J 1993 *IEEE Trans. Appl. Supercond.* **3** 1390
[21] Bean C P 1964 Magnetization of high-field superconductors *Rev. Mod. Phys.* **36** 31
[22] Campbell A M 2017 *Supercond. Sci. Technol.* **30** 125015
[23] Li Q, Yao M, Jiang Z, Bumby C W and Amemiya N 2018 *IEEE Trans. Appl. Supercond.* **28** 6600106
[24] Ainslie M D, Bumby C W, Jiang Z, Toyomoto R and Amemiya N 2018 *Supercond. Sci. Technol.* **31** 074003
[25] Hong Z, Campbell A M and Coombs T A 2006 *Supercond. Sci. Technol.* **19** 1246–52
[26] Vanderbemden P *et al* 2007 *Phys. Rev.* B **75** 174515
[27] Ainslie M D *et al* 2011 *Supercond. Sci. Technol.* **24** 045005
[28] Zhang M, Kim J, Pamidi S, Chudy M, Yuan W and Coombs T A 2012 *J. Appl. Phys.* **111** 083902
[29] Geng J *et al* 2016 *Supercond. Sci. Technol.* **29** 035015
[30] Jiang Z, Toyomoto R, Amemiya N, Zhang X and Bumby C W 2017 *Supercond. Sci. Technol.* **30** 03LT01
[31] Jiang Z *et al* 2018 *IEEE Trans. Appl. Supercond.* **28** 8200305